

Neutron-scattering study of the oxypnictide superconductor $\text{LaFeAsO}_{0.87}\text{F}_{0.13}$ Y. Qiu,^{1,2} M. Kofu,³ Wei Bao,^{4,*} S.-H. Lee,³ Q. Huang,¹ T. Yildirim,¹ J. R. D. Copley,¹ J. W. Lynn,¹ T. Wu,⁵ G. Wu,⁵ and X. H. Chen⁵¹*NIST Center for Neutron Research, National Institute of Standards and Technology, Gaithersburg, Maryland 20899, USA*²*Department of Materials Science and Engineering, University of Maryland, College Park, Maryland 20742, USA*³*Department of Physics, University of Virginia, Charlottesville, Virginia 22904, USA*⁴*Los Alamos National Laboratory, Los Alamos, New Mexico 87545, USA*⁵*Hefei National Laboratory for Physical Science at Microscale and Department of Physics, University of Science and Technology of China, Hefei, Anhui 230026, China*

(Received 6 May 2008; revised manuscript received 14 June 2008; published 26 August 2008)

The recently discovered superconductor $\text{LaO}_{0.87}\text{F}_{0.13}\text{FeAs}$ ($T_C \approx 26$ K) was investigated using the neutron-scattering technique. No spin-density-wave (SDW) order was observed in the normal state or in the superconducting state, both with and without an applied magnetic field of 9 T, consistent with the proposal that SDW and superconductivity are competing in the laminar materials. While our inelastic measurements offer no constraint on the spin dynamic response from a d -wave pairing, an upper limit for the magnetic-resonance peak predicted from an extended s -wave pairing mechanism is provided. Our measurements also support the energy scale of the calculated phonon spectrum, which is used in the electron-phonon coupling theory and fails to produce the high observed T_C .

DOI: [10.1103/PhysRevB.78.052508](https://doi.org/10.1103/PhysRevB.78.052508)

PACS number(s): 74.70.-b, 61.05.fg, 74.25.Ha

I. INTRODUCTION

A family of superconductors has been discovered in laminar oxypnictide $\text{La}(\text{O},\text{F})\text{FeP}$ ($T_C \approx 4$ K),¹ LaONiP ($T_C \approx 3$ K),² and $\text{La}(\text{O},\text{F})\text{FeAs}$ ($T_C \approx 26$ K).³ Enormous excitement has been generated since T_C was raised above 40 K when La was replaced by lanthanide Sm ($T_C \approx 43$ K),⁴ Ce ($T_C \approx 41$ K),⁵ Nd ($T_C \approx 52$ K),⁶ or Pr ($T_C \approx 52$ K) (Ref. 7) in $\text{Ln}(\text{O},\text{F})\text{FeAs}$. $\text{Gd}(\text{O},\text{F})\text{FeAs}$ is also a superconductor⁸ and its T_C has been raised to 36 K.⁹ So far, $\text{Sm}(\text{O},\text{F})\text{FeAs}$ has the highest $T_C \sim 55$ K in the family of superconductors^{10,11} and the transition temperature is the highest among all superconductors except in some cuprates.

The parent compounds LnOFeAs [$\text{Ln}=\text{La}$,³ Sm,¹¹ Ce,⁵ Nd, and Gd (Ref. 8)] are not superconductors. Instead, a spin-density wave (SDW) due to Fermi-surface nesting develops below ~ 150 K with an associated structural transition from tetragonal to orthorhombic symmetry.¹²⁻¹⁴ In addition to adding electrons in $\text{Ln}(\text{O},\text{F})\text{FeAs}$, removing electrons in $(\text{La},\text{Sr})\text{OFeAs}$ also shifts the Fermi surface out of the nesting condition^{12,15} and leads to superconductors of similarly high T_C .¹⁶ Pressure also strongly affects T_C (Refs. 17 and 18) but initial theoretical calculations do not favor the phonon mechanism.¹⁹⁻²¹ Various theoretical possibilities involving magnetic fluctuations have been proposed.^{19,22-27} In particular, a pronounced resonance peak in the spin excitations is predicted for an extended s -wave superconducting order parameter while d -wave order parameter only modestly enhances spin excitations over the normal-state response.^{27,28}

In this neutron-scattering study, we chose superconducting $\text{La}(\text{O},\text{F})\text{FeAs}$ as our subject. Although other $\text{Ln}(\text{O},\text{F})\text{FeAs}$ have higher T_C , the La compound is the most thoroughly studied and it also avoids complexity caused by magnetic rare-earth elements. Additionally, the superconducting gap in $\text{La}(\text{O},\text{F})\text{FeAs}$ has been estimated at $\Delta_0 \approx 3.7(8)$ meV in infrared,²⁹ specific-heat,³⁰ and point-

contact tunneling³¹ experiments. The experimental values of Δ_0 set the theoretical resonance energy of the extended s -wave superconductivity at the in-plane antiferromagnetic wave vector $Q=(1/2, 1/2, 0)$ and at 5.6 ± 1.3 meV (Ref. 27) within the convenient range of neutron-scattering spectroscopy.

II. EXPERIMENTAL DETAILS

At this moment, only polycrystalline samples of $\text{Ln}(\text{O},\text{F})\text{FeAs}$ are available and an ideal instrument for investigating such samples is the time-of-flight disk chopper spectrometer (DCS) at the National Institute of Standards and Technology Center for Neutron Research. A polycrystalline sample of $\text{LaO}_{0.87}\text{F}_{0.13}\text{FeAs}$ with a mass of 2 g was synthesized by the solid-state reaction.³ The resistivity ρ shown in the inset of Fig. 1 was measured using the standard four-probe method. The superconducting transition starts at $T_C = 26$ K, $d\rho/dT$ peaks at 24 K, and ρ reaches zero at 22 K. The transition is among the narrowest for $\text{La}(\text{O},\text{F})\text{FeAs}$ materials.^{3,29-32} During the neutron-scattering experiments, a cryomagnet controlled the sample temperature and magnetic field. The intensity of magnetic inelastic neutron scattering was normalized to absolute units with incoherent nuclear scattering.

III. RESULTS AND DISCUSSIONS

The observed powder-diffraction spectrum at 1.6 K is shown in Fig. 1. It is well accounted for by the tetragonal ZrCuSiAs structure as indicated by the refined profile also shown in Fig. 1. The sample is of high purity. Only minute impurity peaks are discernible in the diffraction spectrum. Refined structure parameters at 1.6 K are listed in Table I. There is little change in the crystal structure between our sample and $\text{LaO}_{0.92}\text{F}_{0.08}\text{FeAs}$ at a similar temperature.¹³

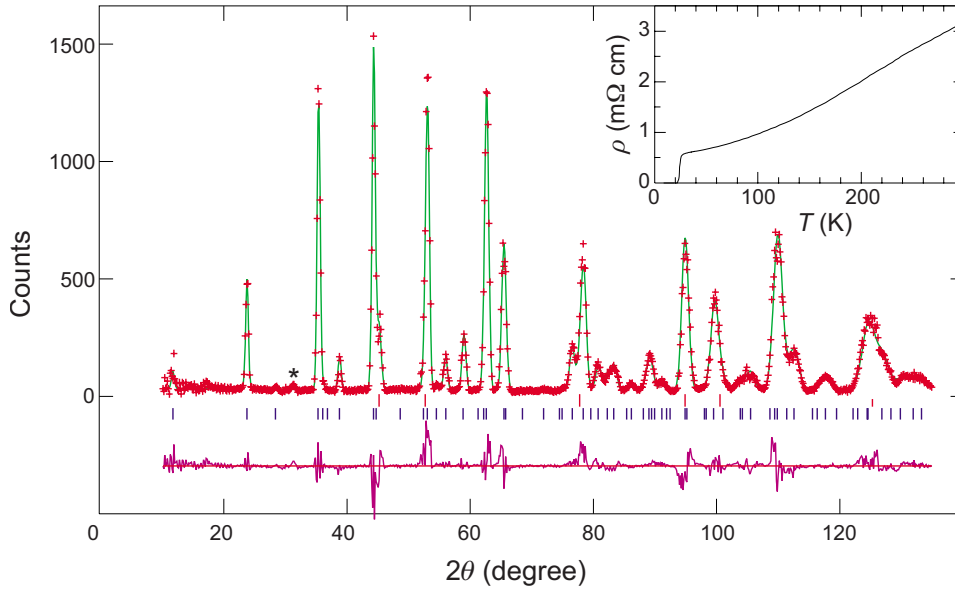


FIG. 1. (Color online) Observed (crosses) and calculated (solid line) neutron powder-diffraction intensities for the superconductor $\text{LaO}_{0.87}\text{F}_{0.13}\text{FeAs}$ at 1.6 K using space-group $P4/nmm$. Vertical lines are Bragg-peak positions for $\text{LaO}_{0.87}\text{F}_{0.13}\text{FeAs}$ (lower) and Al sample holder (upper). The data were collected on DCS with an incident-beam wavelength $\lambda=1.8$ Å. The structure was refined using the GSAS program (Ref. 33). Inset: Resistivity of $\text{LaO}_{0.87}\text{F}_{0.13}\text{FeAs}$ showing the superconducting transition at $T_C=26$ K.

The SDW of LaOFeAs is characterized by the wave vector $(1/2, 1/2, 1/2)$ in terms of the tetragonal $P4/nmm$ unit cell.¹³ The weak staggered magnetic moment $M=0.36(5)\mu_B$ per Fe at 8 K (Ref. 13) can be explained by an associated structure transition.¹⁴ The strongest magnetic Bragg peak $(1/2, 1/2, 3/2)$ is only 1.1% of the intensity of the structural (002) peak.¹³ For superconducting sample $\text{LaO}_{0.92}\text{F}_{0.08}\text{FeAs}$, magnetic peaks of the SDW order are not observed above measurement statistics level of about 0.5% of the (002) peak at 8 K.¹³ Similarly our superconducting sample $\text{LaO}_{0.87}\text{F}_{0.13}\text{FeAs}$ does not show any detectable SDW order down to 1.6 K in the superconducting state (see Fig. 1) or at 30 K in the normal state (see Fig. 2). Applying a magnetic field of 9 T does not induce any magnetic peak stronger than 0.5% of the (002) Bragg peak, the measurement statistics level (see Fig. 2). These results support the proposal that the SDW and superconducting order parameters are competing for itinerant electrons and holes on the Fermi surface^{12,19} in La(O,F)FeAs .

Conventional superconductivity is mediated by phonons and the phonon spectrum has been calculated for La(O,F)FeAs .^{14,15,21} It has been used to calculate the electron-phonon coupling where the T_C from this mechanism is much lower than the observed value.^{19,21} To validate the theoretical calculations, we have measured inelastic neutron scattering from phonons in $\text{LaO}_{0.87}\text{F}_{0.13}\text{FeAs}$ up to 20 meV. For polycrystalline samples, the intensity is given by

TABLE I. Refined structure parameters of $\text{LaO}_{0.87}\text{F}_{0.13}\text{FeAs}$ at 1.6 K. Space group $P4/nmm$ (No. 129). $a=4.0245(3)$ Å, $c=8.713(1)$ Å, $V=141.126(9)$ Å³, $R_p=11.72\%$, and $wR_p=15.53\%$.

Atom	site	x	y	z	$B(\text{Å}^2)$
La	2c	1/4	1/4	0.1442(8)	1.0(2)
Fe	2b	3/4	1/4	1/2	0.3(1)
As	2c	1/4	1/4	0.6541(8)	0.02(2)
O/F	2a	3/4	1/4	0	0.9(2)

$$I(Q, \omega) = \sum_i \frac{\sigma_i \hbar Q^2}{2m_i} \exp(-2W_i) \frac{D_i(\omega)}{\omega} [n(\omega, T) + 1], \quad (1)$$

where σ_i and m_i are the neutron-scattering cross section and atomic mass of the i th atom (La, O/F, Fe, As), $n(\omega, T)$ is the Bose factor, and W_i the Debye-Waller factor.³⁴ Since the weighted phonon density of states (PDOS) given in Eq. (1) is different from the bare PDOS calculated in Refs. 15 and 21, due to different neutron-scattering cross section of elements in $\text{LaO}_{0.87}\text{F}_{0.13}\text{FeAs}$, we have calculated directly the observed PDOS using the phonon eigenvectors calculated in Ref. 14. The results are compared in Fig. 3.

In Fig. 3(a), the measured $I(\omega) = \int dQ I(Q, \omega)$ at 1.6 and 110 K using neutrons of wavelength 1.8 Å integrated from $Q=2.5$ to 7 Å⁻¹ is shown. In Fig. 3(b) the calculated PDOS

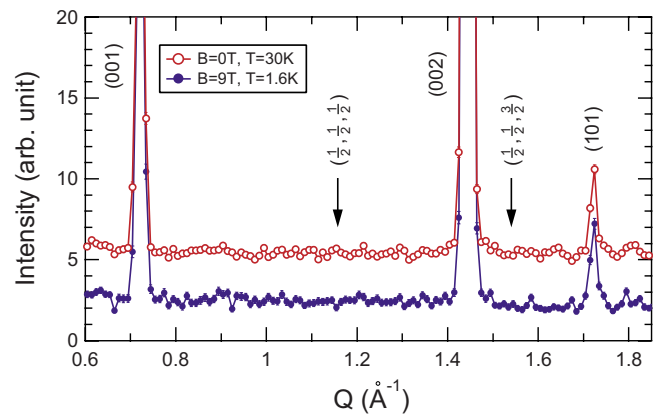


FIG. 2. (Color online) Neutron powder-diffraction intensities of $\text{LaO}_{0.87}\text{F}_{0.13}\text{FeAs}$ at 30 K and zero field in the normal state (open red) and at 1.6 K and 9 T magnetic field in the superconducting state (solid blue). The data are collected with a neutron wavelength $\lambda=4.8$ Å to focus on the small Q range for magnetic signals. The red symbols have been shifted up for clarity. The arrows indicate magnetic Bragg-peak positions of the SDW order. No magnetic peak stronger than 0.5% of the (002) exists in the spectra.

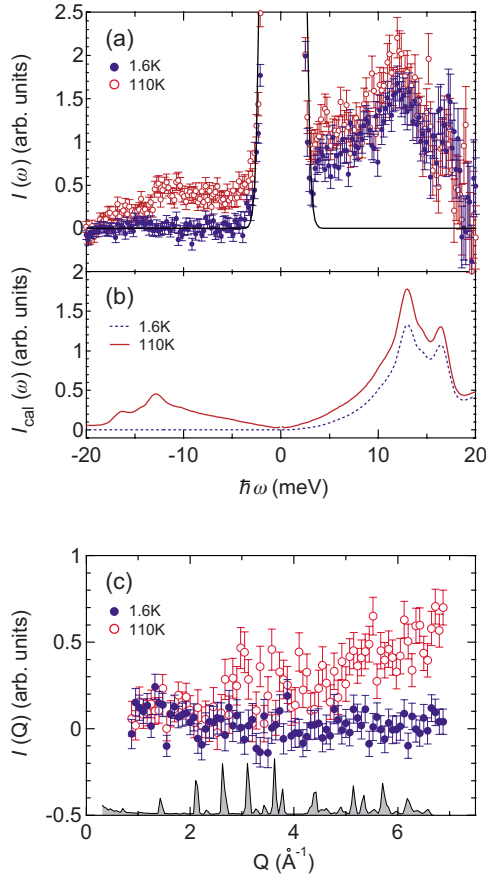


FIG. 3. (Color online) (a) $I(\omega) = \int dQ S(Q, \omega)$ measured at 1.6 and 110 K. The integration range is from 2.5 to 7 \AA^{-1} . (b) Calculated intensity profile at 1.6 and 110 K. (c) Measured $I(Q) = \int d\omega I(Q, \omega)$ at 1.6 and 110 K. The integration range is from -15 to -5 meV. The shaded profile is measured $S(Q, \omega=0)$.

is shown convoluted with instrument resolution. At 1.6 K, the Bose factor leads to zero intensity for negative-energy transfer and measurements there serve to determine the background. The integrated intensity $I(Q) = \int d\omega I(Q, \omega)$ from the negative-energy side (shown in the bottom frame) demonstrates the expected behavior for phonon scattering, which is approximately proportional to $Q^2 I(Q, \omega=0)$.³⁴ The peak positions of the calculated PDOS in Fig. 3(b) are well reproduced in the measured $I(\omega)$ in Fig. 3(a). Thus, the energy scale of the phonon spectra used in the electron-phonon coupling calculations in Refs. 19 and 21, which do not favor the phonon mechanism for superconductivity in La(O,F)FeAs, has experimental support from this work at least below 20 meV.

Unconventional superconductivity mediated by various magnetic channels has been investigated theoretically.^{19,22–27} Both d wave and extended s wave have been proposed for the superconducting order parameter of Ln(O,F)FeAs and the consequences of these pairings in spin dynamics have been investigated theoretically.^{27,28} For d -wave pairing, the superconducting transition only modestly redistributes the spin spectral weight below $2\Delta_0$, where Δ_0 is the superconducting gap parameter. For extended s -wave pairing, a strong resonance peak would appear at the nesting wave vector

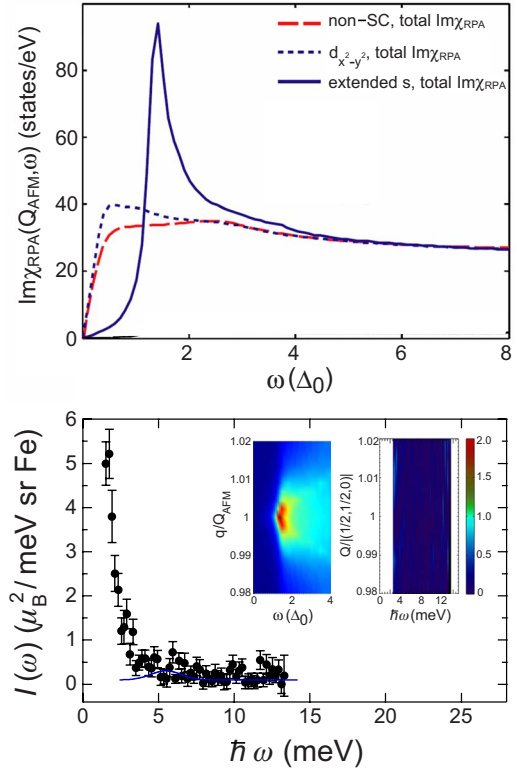


FIG. 4. (Color online) Theoretical $\chi''(Q, \omega)$ in the superconducting state with an extended s -wave order parameter from Ref. 27 is shown in the left inset in the bottom frame. $\chi''(Q_{\text{AFM}}, \omega)$ as a function of ω in the normal and superconducting state with the two order-parameter symmetries (Ref. 27) are shown in the top. Measured $S(Q, \omega) \equiv \chi''(Q, \omega) \langle n(T, \omega) + 1 \rangle / \pi \approx \chi''(Q, \omega) / \pi$ at 1.6 K is shown in the right inset in the bottom frame. The color bar indicates intensity in the units of $\mu_B^2/\text{meV sr Fe}$. $I(\omega) \approx \chi''(Q_{\text{AFM}}, \omega) / \pi$ is shown in the bottom frame.

$Q_{\text{AFM}} = (1/2, 1/2, 0)$ and $\hbar\omega \sim 1.5\Delta_0$. In the top frame of Fig. 4 and the left inset of the bottom frame of Fig. 4, the theoretical imaginary dynamic spin susceptibility $\chi''(Q, \omega)$ from Ref. 27 is shown for various cases. The value of Δ_0 obtained from infrared measurements is between 3.1 and 3.7 meV (Ref. 29) in the specific-heat study at 3.4(5) meV (Ref. 30) and from tunneling at 3.9(7) meV.³¹ Therefore, the resonance peak at Q_{AFM} is between 4.4 and 6.9 meV.

In the right inset of the bottom frame of Fig. 4, magnetic neutron-scattering intensity $S(Q, \omega)$ measured in the superconducting state at 1.6 K is shown in the same (ω, Q) range as in the left inset. Below 2.5 meV, intensity is dominated by incoherent nuclear neutron scattering. The energy dependence at the antiferromagnetic point is shown in the main bottom frame with the same energy scale as in the top frame. Above 2.5 meV, the Bose factor $n(\omega, T) \approx 0$ at 1.6 K. Thus, the measured $S(Q, \omega) \approx \chi''(Q, \omega) / \pi$ can be compared directly to the theoretical $\chi''(Q, \omega)$ in Fig. 4. Powder averaging will enhance the measured intensity at Q larger than $|Q_{\text{AFM}}|$ to some extent; however, the sharp resonance peak will be a little affected.

We did not observe the strongly enhanced superconducting resonance peak in LaO_{0.87}F_{0.13}FeAs at 1.6 K. The upper limit for the intensity of such a resonance peak is 0.5(1)

$\mu_B^2/\text{meV sr per Fe}$ from our data (see the blue curve in the bottom frame). If the predicted resonance peak is as strong as in the unconventional superconductor CeCoIn_5 [$\sim 30\mu_B^2/\text{meV sr per Co}$ (Ref. 35)—being two orders of magnitude stronger than our measurement limit], it would have been observed in our experiments. On the other hand, if the intensity of the resonance peak in $\text{La}(\text{O},\text{F})\text{FeAs}$ is similar to that in $\text{YBa}_2\text{Cu}_3\text{O}_{6+x}$ ($\sim 0.2\mu_B^2/\text{meV sr per Cu}$),³⁶ it would not be observed in our measurements. Theoretically, the peak intensity for the resonance in $\text{La}(\text{O},\text{F})\text{FeAs}$ with the extended s -wave pairing depends on the choice of damping factor and corrections beyond the random-phase approximation.^{27,28} For the d -wave pairing also discussed in Refs. 27 and 28, the modest change in the spin dynamics would be beyond the sensitivity of this polycrystalline experiment.

IV. CONCLUSIONS

In summary, we did not observe the SDW order of LaOFeAs in our superconducting $\text{LaO}_{0.87}\text{F}_{0.13}\text{FeAs}$ sample. The peaks in the theoretical PDOS at 12 and 17 meV are observed in our phonon measurements. The theory of phonon mediated superconductivity, which fails to produce the high $T_C \approx 26$ K, thus is based on reasonable calculated pho-

non spectrum. Our experiments set an upper limit of $0.5\mu_B^2/\text{meV sr per Fe}$ for the resonance peak in the spin excitations at the antiferromagnetic wave vector. Unconventional extended s -wave superconductivity mediated by spin fluctuations is constrained by the limit.

Note added in proof. The nonexistence of the SDW order in the superconducting sample is corroborated by the Mössbauer³⁷ and μSR ^{38,39} measurements. The 12 meV phonon mode has also been observed in optic study⁴⁰ and our phonon DOS results are in general agreement with newer neutron scattering studies.^{41,42}

ACKNOWLEDGMENTS

We would like to thank D. J. Singh and M.-H. Du for their useful communications. Work at LANL is supported by U.S. DOE-OS-BES, at USTC by the Natural Science Foundation of China, Ministry of Science and Technology of China (973 Project No. 2006CB601001) and by the National Basic Research Program of China Contract No. 2006CB922005, at UVA by the U.S. DOE through Contract No. DE-FG02-07ER45384. The DCS at NIST is partially supported by NSF under Agreement No. DMR-0454672.

*wbao@lanl.gov

¹Y. Kamihara *et al.*, *J. Am. Chem. Soc.* **128**, 10012 (2006).

²T. Watanabe, H. Yanagi, T. Kamiya, Y. Kamihara, and H. Hosono, *Inorg. Chem.* **46**, 7719 (2007).

³Y. Kamihara, T. Watanabe, M. Hirano, and H. Hosono, *J. Am. Chem. Soc.* **130**, 3296 (2008).

⁴X. H. Chen, T. Wu, G. Wu, R. H. Liu, H. Chen, and D. F. Fang, *Nature (London)* **453**, 761 (2008).

⁵G. F. Chen *et al.*, *Phys. Rev. Lett.* **100**, 247002 (2008).

⁶Z. A. Ren *et al.*, *Europhys. Lett.* **82**, 57002 (2008).

⁷Z. A. Ren *et al.*, arXiv:0803.4283 (unpublished).

⁸G. F. Chen *et al.*, *Chin. Phys. Lett.* **25**, 2235 (2008).

⁹P. Cheng *et al.*, *Sci. China, Ser. G* **51**, 719 (2008).

¹⁰Z. A. Ren *et al.*, *Chin. Phys. Lett.* **25**, 2215 (2008).

¹¹R. H. Liu *et al.*, arXiv:0804.2105 (unpublished).

¹²J. Dong *et al.*, *Europhys. Lett.* **83**, 27006 (2008).

¹³C. de la Cruz, *et al.*, *Nature (London)* **453**, 899 (2008).

¹⁴T. Yildirim, *Phys. Rev. Lett.* **101**, 057010 (2008).

¹⁵D. J. Singh and M.-H. Du, *Phys. Rev. Lett.* **100**, 237003 (2008).

¹⁶H. H. Wen, G. Xu, L. Fang, H. Yang, and X. Zhu, *Europhys. Lett.* **82**, 17009 (2008).

¹⁷W. Lu, J. Yang, X. L. Dong, Z. A. Ren, G. C. Che, and Z. X. Zhao, *New J. Phys.* **10**, 063026 (2008).

¹⁸B. Lorentz *et al.*, *Phys. Rev. B* **78**, 012505 (2008).

¹⁹I. I. Mazin, D. J. Singh, M. D. Johannes, and M. H. Du, *Phys. Rev. Lett.* **101**, 057003 (2008).

²⁰K. Haule, J. H. Shim, and G. Kotliar, *Phys. Rev. Lett.* **100**, 226402 (2008).

²¹L. Boeri, O. V. Dolgov, and A. A. Golubov, *Phys. Rev. Lett.* **101**, 026403 (2008).

²²K. Kuroki *et al.*, arXiv:0803.3325 (unpublished).

²³X. Dai, Z. Fang, Y. Zhou, and F. Zhang, arXiv:0803.3982 (unpublished).

²⁴Q. Han, Y. Chen, and Z. D. Wang, *Europhys. Lett.* **82**, 37007 (2008).

²⁵H. Eschrig, arXiv:0804.0186 (unpublished).

²⁶P. A. Lee and X. G. Wen, arXiv:0804.1739 (unpublished).

²⁷M. M. Korshunov and I. Eremin, arXiv:0804.1793 (unpublished).

²⁸T. Maier and D. Scalapino, arXiv:0805.0316 (unpublished).

²⁹G. F. Chen, *et al.*, *Phys. Rev. Lett.* **101**, 057007 (2008).

³⁰G. Mu, X. Zhu, L. Fang, L. Shan, C. Ren, and H. H. Wen, *Chin. Phys. Lett.* **25**, 2221 (2008).

³¹L. Shan, Y. Wang, X. Zhu, G. Mu, L. Fang, and H. H. Wen, arXiv:0803.2405 (unpublished).

³²X. Zhu, H. Yang, L. Fang, G. Mu, and H. H. Wen, *Supercond. Sci. Technol.* **21**, 105001 (2008).

³³A. Larson and R. B. Von Dreele, *GSAS: Generalized Structure Analysis System*, 1994.

³⁴R. Osborn, E. A. Goremychkin, A. I. Kolesnikov, and D. G. Hinks, *Phys. Rev. Lett.* **87**, 017005 (2001).

³⁵C. Stock, C. Broholm, J. Hudis, H. J. Kang, and C. Petrovic, *Phys. Rev. Lett.* **100**, 087001 (2008).

³⁶S. M. Hayden, H. A. Mook, P. Dai, T. G. Perring, and F. Doğan, *Nature (London)* **429**, 531 (2004).

³⁷S. Kitao *et al.*, arXiv:0805.0041 (unpublished).

³⁸H. Luetkens *et al.*, arXiv:0804.3115 (unpublished).

³⁹J. P. Carlo *et al.*, arXiv:0805.2186 (unpublished).

⁴⁰S.-L. Drechsler *et al.*, arXiv:0805.1321 (unpublished).

⁴¹A. D. Christianson *et al.*, arXiv:0807.3370 (unpublished).

⁴²R. Mittal *et al.*, arXiv:0807.3172 (unpublished).